MOLECULAR AND CELLULAR BIOLOGY, Nov. 2004, p. 10016–10025 Vol. 24, No. 22
0270-7306/04/$08.00+0 DOI: 10.1128/MCB.24.22.10016–10025.2004
Copyright © 2004, American Society for Microbiology. All Rights Reserved.

Requirement of the Mre11 Complex and Exonuclease 1 for Activation of the Mec1 Signaling Pathway

Daisuke Nakada, Yukinori Hirano, and Katsunori Sugimoto*

Department of Cell Biology and Molecular Medicine, University of Medicine and Dentistry of New Jersey, New Jersey Medical School, Newark, New Jersey

Received 21 June 2004/Returned for modification 11 July 2004/Accepted 22 August 2004

The large protein kinases, ataxia-telangiectasia mutated (ATM) and ATM-Rad3-related (ATR), orchestrate DNA damage checkpoint pathways. In budding yeast, ATM and ATR homologs are encoded by *TEL1* and *MEC1*, respectively. The Mre11 complex consists of two highly related proteins, Mre11 and Rad50, and a third protein, Xrs2 in budding yeast or Nbs1 in mammals. The Mre11 complex controls the ATM/Tel1 signaling pathway in response to double-strand break (DSB) induction. We show here that the Mre11 complex functions together with exonuclease 1 (Exo1) in activation of the Mec1 signaling pathway after DNA damage and replication block. Mec1 controls the checkpoint responses following UV irradiation as well as DSB induction. Correspondingly, the Mre11 complex and Exo1 play an overlapping role in activation of DSB- and UV-induced checkpoints. The Mre11 complex and Exo1 collaborate in producing long single-stranded DNA (ssDNA) tails at DSB ends and promote Mec1 association with the DSBs. The Ddc1-Mec3-Rad17 complex associates with sites of DNA damage and modulates the Mec1 signaling pathway. However, Ddc1 association with DSBs does not require the function of the Mre11 complex and Exo1. Mec1 controls checkpoint responses to stalled DNA replication as well. Accordingly, the Mre11 complex and Exo1 contribute to activation of the replication checkpoint pathway. Our results provide a model in which the Mre11 complex and Exo1 cooperate in generating long ssDNA tracts and thereby facilitate Mec1 association with sites of DNA damage or replication block.

The maintenance of genome stability is critical to the survival and propagation of all cellular organisms. In response to DNA damage, cells activate a complex signaling pathway to promote DNA repair and induce cell cycle arrest. When DNA replication is blocked, cells also activate signaling pathways to facilitate DNA synthesis and prevent entry into M phase. These signaling pathways are called DNA damage or replication checkpoints in eukaryotes (11). These checkpoint pathways transmit signals through evolutionarily conserved protein kinases (1, 64). Two large protein kinases, ataxia-telangiectasia mutated (ATM) and ATM-Rad3-related (ATR), are the central components of the checkpoint pathway in mammalian cells. Whereas ATM responds primarily to double-strand breaks (DSBs) of DNA, ATR functions in responses to DSB induction as well as other types of DNA insults, such as UV-induced lesions and stalled replication. These large kinases regulate the activation of two downstream protein kinases, Chk1 and Chk2.

In the budding yeast *Saccharomyces cerevisiae*, *MEC1* and *TEL1* encode ATR- and ATM-related proteins, respectively. Mec1 responds to a variety of types of DNA damage and plays a central role in DNA damage and replication checkpoint controls (29), whereas Tel1 plays only a minor role in response to DSBs (35, 39, 50). Mec1 physically interacts with Ddc2 (also called Lcd1 and Pie1), a protein related to the mammalian ATR-interacting protein ATRIP (6, 41, 47, 59). Mec1 and Ddc2 function in the form of the Mec1-Ddc2 complex, and both localize to sites of DNA damage and replication block (23, 25, 30, 32, 40, 48). Replication protein A (RPA) binds single-stranded DNA (ssDNA), which is generated during DNA repair and replication processes (61). Recent evidence supports a model in which Ddc2 recognizes DNA damage by interacting with RPA-coated ssDNA and enables the Mec1-Ddc2 complex to associate with sites of DNA damage (65). Similar to Mec1, Tel1 localizes to DSB lesions (38). However, whether the Tel1 localization requires RPA function is not known. Kinases related to mammalian Chk1 and Chk2 are called Chk1 and Rad53, respectively, in budding yeast (64). Rad53 plays a critical role in checkpoint responses to DNA damage throughout the cell cycle as well as DNA replication block (29), whereas Chk1 acts at least in part at G_2/M (49). After DNA damage or replication block, Rad53 becomes phosphorylated and activated in a Mec1- and Tel1-dependent manner (39, 50, 58). Rad53 activation leads to cell cycle arrest and transcription of genes required for DNA synthesis and repair (11, 29). Chk1 is phosphorylated after DNA damage as well, and its phosphorylation requires Mec1 function (49).

Phosphorylation and activation of Rad53 are also dependent on *DDC1*, *MEC3*, *RAD17*, and *RAD24* (29). The Ddc1, Mec3, and Rad17 proteins are homologous to the mammalian Rad9, Hus1, and Rad1, respectively, and are all structurally related to PCNA (64). Rad24, a mammalian Rad17 homolog, is structurally similar to components of replication factor C (RFC) (64). Ddc1, Mec3, and Rad17 form a PCNA-related complex (64), whereas Rad24 forms an RFC-related complex with Rfc2, Rfc3, Rfc4, and Rfc5 (17, 36). The Rad24 complex regulates the recruitment of the Ddc1 complex to sites of DNA damage (25, 32). Localization of the Ddc1 complex to sites of DNA damage is also dependent on RPA function (66). The Rad24 and Ddc1 complexes play crucial roles in the activation of the

* Corresponding author. Mailing address: Department of Cell Biology and Molecular Medicine, New Jersey Medical School, 185 S. Orange Ave., Newark, NJ 07103. Phone: (973) 972-4034. Fax: (973) 972-7489. E-mail: sugimoka@umdnj.edu.

Mec1 signaling pathway (29) but appear to function in parallel with the Tel1 pathway (56).

The Mre11 complex consists of two highly conserved proteins, Mre11 and Rad50, and a third protein, either Xrs2 in budding yeast or Nbs1 in mammals (8, 20). The Mre11 complex mediates diverse functions in several aspects of DNA metabolism, including DSB repair and telomere maintenance. The Mre11 complex is implicated in two different repair processes of DSB: homologous recombination and nonhomologous end joining. In DSB processing, the Mre11 complex is primarily involved in the generation of the 3′ ssDNA tails. Exonuclease 1 (Exo1) is highly conserved among eukaryotes and possesses 5′ to 3′ double-stranded DNA (dsDNA) exonuclease activity (13, 52). In budding yeast, Exo1 acts in concert with the Mre11 complex in DNA repair and homologous recombination (34, 54). Although the Mre11 complex behaves as 5′ to 3′ exonuclease in vivo, Mre11 orthologs have 3′ to 5′ dsDNA exonuclease and ssDNA endonuclease activities in vitro (8, 20). Moreover, nuclease-deficient *mre11* mutants show the wild-type level of DSB processing in mitosis (33). Thus, how nuclease activities of the Mre11 complex contribute to ssDNA accumulation remains to be determined.

In addition to DSB repair, the Mre11 complex is required for checkpoint responses after DSB induction (8). Studies of mammalian cells have established that the Mre11 complex controls the ATM signaling pathway (22, 43). Mutations in ATM lead to ataxia-telangiectasia, and cells from these patients are hypersensitive to DSB-inducing agents and defective in the checkpoint activation. Hypomorphic mutations in Mre11 and Nbs1 cause ataxia-telangiectasia-like disease and Nijmegen breakage syndrome, respectively, disorders that are phenotypically similar to ataxia-telangiectasia. ATM activation correlates with autophosphorylation on Ser 1981 (2), and this phosphorylation requires functions of the Mre11 complex (4, 57). Recent evidence suggests that the Mre11 complex modulates the substrate recognition of ATM by direct interaction (26). Furthermore, the Mre11 complex controls the accumulation of ATM at DSB lesions (24). In budding yeast, the Mre11 complex controls the Tel1 signaling pathway (9, 56). Tel1 interacts with Xrs2 in a manner dependent on the Xrs2 C terminus (38). The C-terminal truncation impairs the Tel1 localization to DSBs and diminishes Tel1-dependent signaling (38). Thus, the functions of ATM/Tel1 and the Mre11 complex in the cellular DNA damage response are conserved between mammals and budding yeast. Although the Mre11 complex is required for activation of the ATM/Tel1 signaling pathway, it does control the ATM/Tel1-independent pathway. For example, in budding yeast, the Mre11 complex is essential for cell survival after DNA damage (8, 20), but no apparent survival defect is associated with *tel1*Δ mutation (35, 39, 50). Furthermore, the Mre11 complex is required for the G_2/M-phase DNA damage checkpoint after DSB induction (19), whereas Tel1 contributes little to the checkpoint responses (39).

In this study, we show that the Mre11 complex functions in concert with Exo1 to activate the Mec1 signaling pathway. The Mre11 complex and Exo1 collaborate in ssDNA accumulation at DSB ends and promote Mec1 association with DSBs. In contrast, the Mre11 complex and Exo1 are dispensable for Ddc1 association with DSBs. The Mre11 complex and Exo1 are not only required for checkpoint responses to DSBs but are also involved in checkpoint activation after UV irradiation. Moreover, they contribute to activation of DNA replication checkpoints as Mec1 does. We propose a model in which the Mre11 complex and Exo1 cooperate in generating long ssDNA tails and thereby facilitate Mec1 association with sites of DNA damage or stalled replication.

TABLE 1. Strains used in this study[a]

Strain	Genotype
KSC1560	*sml1*Δ::*LEU2*
KSC1562	*xrs2*Δ::*hisG sml1*Δ::*LEU2*
KSC1563	*xrs2-11*::*KanMX sml1*Δ::*LEU2*
KSC1661	*tel1*Δ::*KanMX sml1*Δ::*LEU2*
KSC1561	*mec1*Δ::*LEU2 sml1*Δ::*LEU2*
KSC1620	*xrs2*Δ::*hisG*
KSC1933	*mre11*Δ::*hisG*
KSC1846	*exo1*Δ::*URA3*
KSC1979	*xrs2*Δ::*hisG exo1*Δ::*URA3*
KSC1980	*mre11*Δ::*hisG exo1*Δ::*URA3*
KSC1982	*rfa1-t11*
KSC1983	*rfa1-t11 xrs2*Δ::*hisG*
KSC1512	*MEC1-HA*::*TRP1*
KSC1632	*MEC1-HA*::*TRP1 xrs2*Δ::*hisG*
KSC1633	*MEC1-HA*::*TRP1 exo1*Δ::*URA3*
KSC1634	*MEC1-HA*::*TRP1 xrs2*Δ::*hisG exo1*Δ::*URA3*
KSC1984	*MEC1-HA*::*TRP1 rfa1-t11*
KSC1985	*MEC1-HA*::*TRP1 rfa1-t11 xrs2*Δ::*hisG*
KSC1637	*DDC1-HA*::*TRP1*
KSC1638	*DDC1-HA*::*TRP1 xrs2*Δ::*hisG*
KSC1639	*DDC1-HA*::*TRP1 exo1*Δ::*URA3*
KSC1640	*DDC1-HA*::*TRP1 xrs2*Δ::*hisG exo1*Δ::*URA3*
KSC1986	*DDC1-HA*::*TRP1 rfa1-t11*
KSC1987	*DDC1-HA*::*TRP1 rfa1-t11 xrs2*Δ::*hisG*

[a] All the strains are isogenic to KSC1516 (*MAT***a**-*inc ADH4cs*::*HIS2 ade1 his2 leu2 trp1 ura3*) (37).

MATERIALS AND METHODS

Plasmids and strains. To express the HA-tagged Chk1 protein, the DNA sequences encoding the HA epitopes were attached in frame to the C-terminus end of Chk1. The entire region of *CHK1*, lacking the termination codon and the 3′-untranslated region, was amplified by PCR. The *CHK1-HA* plasmid (YCpT-CHK1-HA) was constructed by ligation of the EcoRI-BglII-treated PCR fragment and a BamHI-SalI fragment encoding four hemagglutinin (HA) epitopes with an EcoRI-SalI-linearized YCplac22 (16). The plasmids to construct *mre11*Δ and *exo1*Δ mutations were obtained from H. Tsubouchi, H. Ogawa, and T. Ogawa (54). YCpA-GAL-HO and YCpT-RAD53-HA were previously described (38). Cells carrying the *rfa1-t11* mutation (55) were obtained by transforming the pKU2-t11 plasmid (obtained from K. Umezu and R. Kolodner) after linearization by PCR. Other strain constructs were described elsewhere (25, 37, 38, 59). All the strains used in this study are isogenic to KSC1516 (37) and are listed in Table 1.

Immunoblotting. Immunoblotting was performed as described previously (37). To examine Rad53 phosphorylation after exposure to phleomycin or UV light, cells carrying YCpT-RAD53-HA were grown in yeast extract-peptone-dextrose (YEPD) and then arrested at G_1 or G_2/M after a 2-h incubation with 6 μg of α-factor/ml or 15 μg of nocodazole/ml, respectively. After arrest, cells were treated with 50 μg of phleomycin/ml in the presence of α-factor or nocodazole. Alternatively, cells were spread out on YEPD plates and immediately irradiated with a 254-nm UV lamp at 75 J/m^2. After UV irradiation, cells were released into fresh YEPD medium containing α-factor or nocodazole. To examine Rad53 phosphorylation after hydroxyurea (HU) treatment, cells were arrested at G_1 after incubation with 6 μg of α-factor/ml for 2 h and then released into medium containing 10-mg/ml HU. To examine the HO-induced Rad53 phosphorylation, cells carrying YCpA-GAL-HO and YCpT-RAD53-HA were grown in selective medium containing sucrose and then arrested with 15 μg of nocodazole/ml for 2 h at G_2/M. To induce *HO* expression, galactose was added to the culture to 2% at a final concentration. Cells carrying YCpT-CHK1-HA were treated similarly to monitor the phosphorylation status of Chk1.

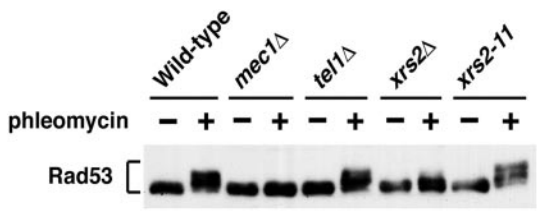

FIG. 1. Effect of *mec1*Δ, *tel1*Δ, or *xrs2* mutations on phleomycin-induced Rad53 phosphorylation. Cells carrying YCpT-RAD53-HA were arrested at G_2/M with nocodazole, and untreated (−) or treated (+) with phleomycin, maintaining the G_2/M arrest for 60 min. Cells were then collected and subjected to immunoblotting analysis with anti-HA antibodies. Strains used are wild type (KSC1560), *mec1*Δ (KSC1561), *tel1*Δ (KSC1661), *xrs2*Δ (KSC1562), and *xrs2-11* (KSC1563). All the strains contain an *sml1*Δ mutation that suppresses the lethality of *mec1*Δ mutants (63).

Phleomycin and UV synchrony experiments and cell survival assays. Phleomycin and UV synchrony experiments were performed as previously described (39, 59). Log-phase cultures were arrested with 15-μg/ml nocodazole for 2 h to synchronize cells at G_2/M. For exposure to phleomycin, cells were incubated with 50-μg/ml phleomycin for 1 h. Cells were then washed to remove both nocodazole and phleomycin and released in fresh YEPD. For exposure to UV light, cells arrested at G_2/M were spread on YEPD plates and irradiated with a 254-nm UV lamp at 75 J/m^2. Cells were then washed to remove nocodazole and released into fresh YEPD. At timed intervals, cells were withdrawn and stained with DAPI (4′,6′-diamidino-2-phenylindole) for microscopic examination. Cell viability after exposure to phleomycin or UV light was determined as described previously (39, 59).

Measurement of DSB processing rate. DNA degradation at DSB ends was monitored as previously described (37, 38). To prepare strand-specific probes, DNA fragments were amplified from genomic DNA by PCR with oligonucleotide primers flanked by a T7 promoter sequence. The sequences of the oligonucleotides are available upon request. ^{32}P-labeled RNA probes were synthesized with T7 RNA polymerase.

ChIP assay. The chromatin immunoprecipitation (ChIP) assay was performed essentially as described previously (38). Anti-HA (12CA5) antibodies and 0.1% sodium deoxycholate were replaced by anti-HA (16B2) antibodies and 0.05% sodium dodecyl sulfate, respectively. PCR was performed in a nonsaturating condition, in which the rate of PCR amplification is proportional to the concentration of substrate and cycling.

Immunofluorescence microscopic analysis. The culture was synchronized in the G_1 phase by addition of 6-μg/ml α-factor for 2 h. Cells were then washed to remove α-factor and released into YEPD containing 10-mg/ml HU. Aliquots of cells were removed and processed for indirect immunofluorescence microscopy as described previously (59).

RESULTS

Phleomycin-induced Rad53 phosphorylation in cells carrying *tel1*, *xrs2*, or *mec1* mutations. To further understand the functional link between the Mre11 complex and Tel1, we compared Rad53 phosphorylation in *xrs2*, *tel1*Δ, and *mec1*Δ mutants after DNA damage (Fig. 1). Phosphorylation of Rad53 can be detected as slower-migrating forms on immunoblots. Cells expressing HA-tagged Rad53 were arrested at G_2/M phase with nocodazole and then incubated with the DSB-inducing agent phleomycin. After treatment with phleomycin, cells were subjected to immunoblotting analysis with anti-HA antibodies. Whereas *xrs2*Δ mutants exhibited a partial defect in Rad53 phosphorylation compared with wild-type cells, no phosphorylation defect was observed in *tel1*Δ mutants (39). The *xrs2-11* mutation confers the same phenotype as *tel1*Δ mutation (38). Consistently, efficient phosphorylation was detected in *xrs2-11* mutants. In contrast, *mec1*Δ mutants showed a significant phosphorylation defect (39). These results raise a possibility that the Mre11 complex may function in the same signaling pathway as Mec1 does.

Effect of *exo1*Δ mutation in combination with *xrs2*Δ or *mre11*Δ mutation on cellular responses to phleomycin-induced DNA damage. Exo1 possesses a 5′ to 3′ exonuclease activity and acts redundantly with the Mre11 complex in homologous recombination and other aspects of DNA damage metabolism (34, 54). We therefore investigated whether the Mre11 complex and Exo1 cooperate in checkpoint responses to phleomycin-induced DNA damage. We first tested the effect of *exo1*Δ mutation on cell survival of *xrs2*Δ or *mre11*Δ mutants after phleomycin treatment (Fig. 2A). The introduction of *exo1*Δ mutation exacerbated sensitivity of *xrs2*Δ and *mre11*Δ mutants to phleomycin, although the *exo1*Δ single mutation did not confer sensitivity. We then monitored the phosphorylation status of Rad53 in *xrs2*Δ *exo1*Δ and *mre11*Δ *exo1*Δ double mutants after phleomycin treatment at the G_2/M phase (Fig. 2B). Rad53 was phosphorylated in *exo1*Δ mutants as efficiently as in wild-type cells. However, its phosphorylation was decreased in *xrs2*Δ or *mre11*Δ single mutants and was not detected in *xrs2*Δ *exo1*Δ or *mre11*Δ *exo1*Δ double mutants. No difference in Rad53 phosphorylation was observed in cells carrying *mre11*Δ or *xrs2*Δ mutations, consistent with the current view that Mre11, Rad50, and Xrs2 form a complex and function together (8, 20). In addition to Rad53, Chk1 controls the G_2/M-phase DNA damage checkpoint pathway (49). We then monitored Chk1 phosphorylation after phleomycin treatment (Fig. 2C). Chk1 was phosphorylated in wild-type and *exo1*Δ mutants, whereas its phosphorylation was undetectable in *xrs2*Δ single or *xrs2*Δ *exo1*Δ double mutants.

We next examined the cell cycle arrest after exposure to phleomycin in *xrs2*Δ, *exo1*Δ, and their double mutants by monitoring mitotic division (Fig. 2D). When cell cultures were released from nocodazole arrest after phleomycin treatment, wild-type cells showed delayed nuclear division. Meanwhile, *xrs2*Δ single mutants proceeded through mitosis slightly faster than wild-type cells. Although *exo1*Δ mutation alone did not affect the process, its introduction further accelerated the mitotic progression in *xrs2*Δ mutants. We previously showed that *mec1*Δ mutants are defective in the mitotic delay after phleomycin treatment, whereas no apparent defect is associated with *tel1*Δ mutation (39). As a control, we also analyzed the mitotic progression in *mec1*Δ mutants (Fig. 2D). Similar defects were found in *mec1*Δ single and *xrs2*Δ *exo1*Δ double mutants.

Previous results indicated that the Mre11 complex is involved in checkpoint responses to DSB induction at G_1 phase as well (19). We then monitored the phosphorylation status of Rad53 in G_1-arrested *xrs2*Δ *exo1*Δ double mutants after phleomycin treatment (Fig. 2E). Again, Rad53 was phosphorylated in *exo1*Δ mutants as efficiently as in wild-type cells, whereas phosphorylation was partially decreased in *xrs2*Δ single mutants. Phosphorylation was further decreased in *xrs2*Δ *exo1*Δ double mutants. Together, these results indicate that the Mre11 complex collaborates with Exo1 in activating the Mec1-dependent checkpoint pathway after phleomycin treatment.

Effect of *xrs2*Δ and *exo1*Δ mutations on Mec1 and Ddc1 association with DSBs. Mec1 forms a complex with Ddc2 (41, 47, 59), and the Mec1-Ddc2 complex localizes to sites of DNA damage (25, 32, 48). Rad24 forms an RFC-related complex and recruits the Ddc1-Mec3-Rad17 complex to DNA lesions

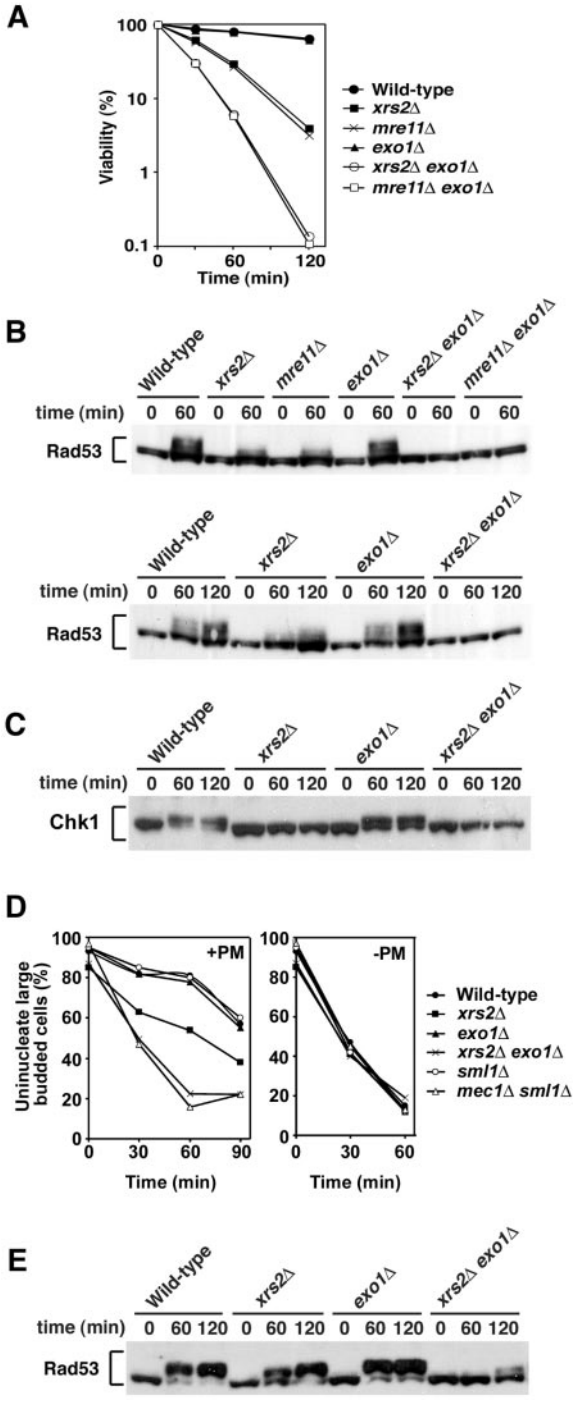

FIG. 2. Overlapping function of the Mre11 complex and Exo1 in response to phleomycin-induced DNA damage. (A) Effect of *mre11*Δ, *xrs2*Δ, and *exo1*Δ mutations on cell viability after exposure to phleomycin. Cells were grown in log phase and incubated with phleomycin. At the indicated times, aliquots of cells were collected and the viability was estimated. Strains used are wild type (KSC1516), *mre11*Δ (KSC1933), *xrs2*Δ (KSC1562), *exo1*Δ (KSC1846), *mre11*Δ *exo1*Δ (KSC1980), and *xrs2*Δ *exo1*Δ (KSC1979). (B) Effect of *mre11*Δ, *xrs2*Δ, and *exo1*Δ mutations on phleomycin-induced Rad53 phosphorylation at G_2/M. Cells carrying YCpT-RAD53-HA were arrested with nocodazole and incubated with phleomycin maintaining the arrest. Cells were then collected at the indicated time and analyzed as in Fig. 1 to detect Rad53 phosphorylation. Strains used are the same as in panel A. (C) Effect of *mre11*Δ, *xrs2*Δ, and *exo1*Δ mutations on phleomycin-induced Chk1 phosphorylation at G_2/M. Cells carrying YCpT-CHK1-HA were analyzed as in panel B to detect Chk1 phosphorylation. Strains used are wild type (KSC1516), *xrs2*Δ (KSC1562), *exo1*Δ (KSC1846), and *xrs2*Δ *exo1*Δ (KSC1979). (D) Cell cycle progression delay after phleomycin treatment in G_2/M phase. Cells were synchronized with nocodazole at G_2/M and then treated with phleomycin (+PM) or untreated (−PM). At the indicated times after release from nocodazole, the percentage of uninucleate large-budded cells was scored after DAPI staining. Strains used are wild type (KSC1516), *xrs2*Δ (KSC1562), *exo1*Δ (KSC1846), *xrs2*Δ *exo1*Δ (KSC1979), *sml1*Δ (KSC1560), and *mec1*Δ *sml1*Δ (KSC1561). (E) Effect of *mre11*Δ, *xrs2*Δ, and *exo1*Δ mutations on phleomycin-induced Rad53 phosphorylation at G_1. Cells carrying YCpT-RAD53-HA were arrested with α-factor and incubated with phleomycin maintaining the arrest. Cells were then collected at the indicated time and analyzed as in panel B. Strains used are the same as in panel C.

(25, 32). Although the Mec1 and Ddc1 complexes are independently recruited to DNA lesions (25, 32), the activation of the Mec1 signaling pathway requires functions of the Rad24 and Ddc1 complexes (29). It is thus possible that the Mre11 complex and Exo1 control localization of the Mec1 and Ddc1 complexes to DNA lesions. To address this possibility, we examined the association of Mec1 and Ddc1 with the HO-induced DSB in *xrs2*Δ and *exo1*Δ mutants by ChIP assay. HO is a sequence-specific endonuclease that generates DSB. We used an experimental system in which cells contain a single HO cleavage site at the *ADH4* locus (Fig. 3A), and HO is expressed from GAL-HO plasmid after incubation with galactose (38). The HO-induced DSB at the *ADH4* locus is not efficiently repaired by homologous recombination and thereby activates the DNA damage checkpoint pathway at G_2/M but not at G_1 (42, 53).

We first monitored Rad53 phosphorylation after *HO* expression in *xrs2*Δ and *exo1*Δ mutants (Fig. 3B). Cells expressing Rad53-HA were transformed with the GAL-HO plasmid. Transformed cells were grown initially in sucrose to repress *HO* expression and then transferred to medium containing nocodazole to arrest at G_2/M. After arrest, galactose was added to induce *HO* expression. Cells were collected at various times and subjected to immunoblotting analysis. Rad53 was phosphorylated in *exo1*Δ single mutants as efficiently as in wild-type cells. However, phosphorylation was partially decreased in *xrs2*Δ mutants and was not detectable in *xrs2*Δ *exo1*Δ double mutants. Thus, similar to phleomycin-induced lesions, HO-induced DSBs activate checkpoint responses in an Xrs2- and Exo1-dependent manner.

DSB ends are degraded primarily by 5′ to 3′ exonuclease activities, generating 3′-ended single-stranded DNA tails (60). To confirm an overlapping role of the Mre11 complex and Exo1 in DSB processing, we monitored the DNA degradation rate at DSB ends after *HO* expression in *xrs2*Δ and *exo1*Δ mutant cells (Fig. 3C). Cells carrying the GAL-HO plasmid were grown as above to induce *HO* expression. After *HO* expression, cells were collected at various times to prepare genomic DNA. Purified DNA was fixed to membrane filters and hybridized with strand-specific RNA probes complementary to sequences near the cleavage site at the *ADH4* locus (38). The rate of 5′ to 3′ degradation of the DNA ends was partially decreased in *xrs2*Δ mutants as found previously (21, 38), whereas no degradation defect was observed in *exo1*Δ mutants. Degradation was much slower in *xrs2*Δ *exo1*Δ double

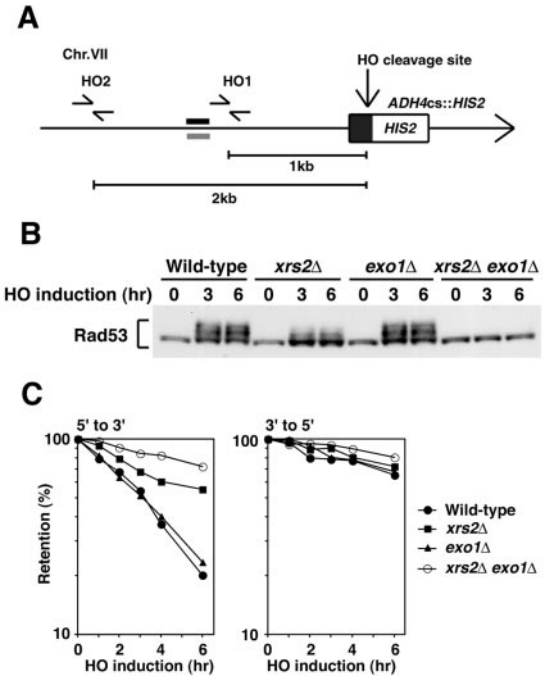

FIG. 3. Effect of *xrs2*Δ and *exo1*Δ mutations on cellular responses to DSBs. (A) Schematic of the HO cleavage site at the *ADH4* locus (*ADH4*cs). An HO cleavage site, marked with *HIS2*, was introduced at the *ADH4* locus on chromosome VII. The primer pairs were designed to amplify regions 1 and 2 kb apart from the HO cleavage site. An arrow represents the telomere. The black and gray bars indicate probes to examine the rate of degradation of the DSB ends (38). (B) Rad53 phosphorylation in response to HO-induced DSBs. Cells carrying YCpT-RAD53-HA and YCpA-GAL-HO were grown in sucrose and treated with nocodazole. After arrest at G_2/M, the culture was incubated with galactose to induce *HO* expression. Aliquots were harvested at the indicated time points and analyzed as in Fig. 1. Strains used are wild type (KSC1516), *exo1*Δ (KSC1846), *xrs2*Δ (KSC1562), and *xrs2*Δ *exo1*Δ (KSC1979). (C) Degradation of the HO-induced DSB ends. Wild-type (KSC1516), *exo1*Δ (KSC1846), *xrs2*Δ (KSC1562), and *xrs2*Δ *exo1*Δ (KSC1979) cells carrying YCpA-GAL-HO were treated as in panel B. Purified DNAs were fixed to a membrane and hybridized with RNA probes, each complementary to the 5′- to 3′- or 3′- to 5′-degrading strand.

mutants than in *xrs2*Δ single mutants, although some residual degradation was observed in the double mutants. In contrast, *xrs2*Δ, *exo1*Δ, and their double mutations had little effect on the 3′ to 5′ degradation. DSB induction by HO does not require the functions of the Mre11 complex and Exo1 (54). These results indicate that the Mre11 complex and Exo1 collaborate in the ssDNA generation at DSB ends, consistent with the previous findings that they play an overlapping role in DNA damage repair (34, 54).

We then tested whether Mec1 associates with the HO-induced DSB in *xrs2*Δ and *exo1*Δ mutants by ChIP assay (Fig. 4A). Cells expressing HA-tagged Mec1 were transformed with the GAL-HO plasmid and grown as above to induce *HO* expression. Cells were collected at various times, and extracts prepared after formaldehyde cross-linking were sonicated and subjected to immunoprecipitation with anti-HA antibodies. Coprecipitated DNA was extracted and amplified by PCR using a primer set corresponding to regions near the HO restriction site or primers for the *SMC2* locus containing no cleavage site. As found previously (25, 38), Mec1 associated with the HO-induced DSB in wild-type cells; PCR amplified sequences near the HO restriction site after incubation with galactose but not a control site in the *SMC2* locus. Mec1 associated with the DSB efficiently in *exo1*Δ single mutants as well. However, the Mec1 association was partially decreased in *xrs2*Δ single mutants and was undetectable in *xrs2*Δ *exo1*Δ double mutants. We also examined Ddc1 association with the HO-induced DSB in those *xrs2*Δ and *exo1*Δ mutants (Fig. 4B). Cells expressing HA-tagged Ddc1 were transformed with the GAL-HO plasmid and were examined as above by ChIP assay. Similar to the Mec1 association, Ddc1 association with DSBs occurred efficiently in *exo1*Δ single mutants. However, unlike the Mec1 association, the Ddc1 association was neither affected by *xrs2*Δ single nor *xrs2*Δ *exo1*Δ double mutation. Thus, Mec1 association with DSBs correlates with the length of ssDNA at the DSB ends, whereas the generation of long ssDNA tracts is not critical for the Ddc1 association.

Synergetic effect of *rfa1-t11* and *xrs2*Δ mutations on Mec1 and Ddc1 association with DSBs. Single-stranded regions of DNA are covered with RPA that acts in most aspects of cellular DNA metabolism (61). RPA is composed of three subunits that are encoded by *RFA1*, *RFA2*, and *RFA3*. Recent evidence provided a model in which the RPA-coated ssDNA is an important structure to recruit the Mec1-Ddc2 and Ddc1-Mec3-Rad17 complexes to sites of DNA damage (65, 66). A mutation in *RFA1*, *rfa1-t11*, impairs association of the Mec1 and Ddc1 complexes with DNA lesions but does not affect binding of RPA to ssDNA (65). It was possible that limited ssDNA generation would further decrease association of Mec1 and Ddc1 with DSBs in *rfa1-t11* mutants. We then compared

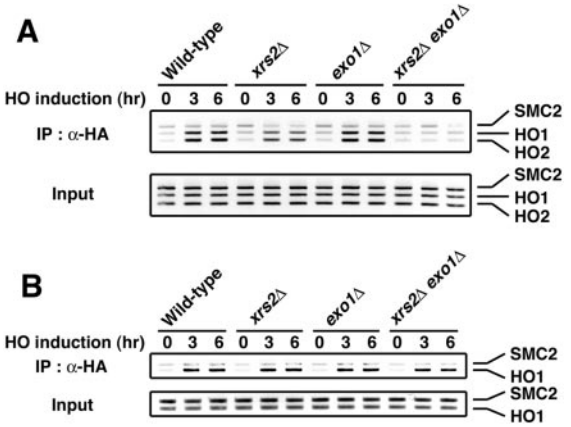

FIG. 4. Effect of *xrs2*Δ and *exo1*Δ mutations on association of Mec1 and Ddc1 with the HO-induced DSB. (A) Association of Mec1 with DSBs. Cells expressing HA-tagged Mec1 were transformed with YCpA-GAL-HO plasmid. Transformed cells were grown in sucrose and treated with nocodazole. After arrest at G_2/M, the culture was incubated with galactose to induce *HO* expression, while part of the culture was maintained in sucrose to repress *HO* expression. Aliquots of cells were collected at the indicated times and subjected to chromatin immunoprecipitation. PCR was carried out with the primers for the HO cleavage site at the *ADH4* locus and for the control *SMC2* locus (see Fig. 3A). PCR products from the respective input extracts are shown below. Strains used here are wild type (KSC1512), *exo1*Δ (KSC1633), *xrs2*Δ (KSC1632), and *xrs2*Δ *exo1*Δ (KSC1634). (B) Association of Ddc1 with the HO-induced DSB. Cells expressing Ddc1-HA were analyzed as in panel A. Strains used here are wild type (KSC1637), *xrs2*Δ (KSC1638), *exo1*Δ (KSC1639), and *xrs2*Δ *exo1*Δ (KSC1640).

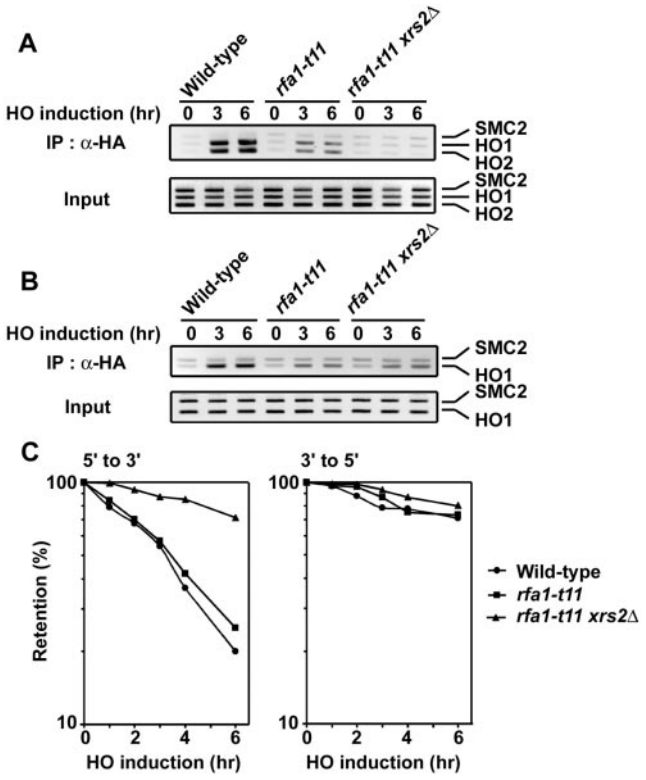

FIG. 5. Effect of *rfa1-t11* mutation on DSB association of Mec1 and Ddc1 in *xrs2*Δ mutants. (A) Association of Mec1 with DSBs. Cells expressing Mec1-HA were analyzed as in Fig. 4A. Strains used here are wild type (KSC1512), *rfa1-t11* (KSC1984), and *rfa1-t11 xrs2*Δ (KSC1985). (B) Association of Ddc1 with the HO-induced DSB. Cells expressing Ddc1-HA were analyzed as in panel A. Strains used here are wild type (KSC1637), *rfa1-t11* (KSC1986), and *rfa1-t11 xrs2*Δ (KSC1987). (C) Degradation of the HO-induced DSB ends. Wild-type (KSC1516), *rfa1-t11* (KSC1982), and *rfa1-t11 xrs2*Δ (KSC1983) cells carrying YCpA-GAL-HO were analyzed as in Fig. 3C.

association of Mec1 and Ddc1 with the HO-induced DSB in *rfa1-t11* single and *rfa1-t11 xrs2*Δ double mutants (Fig. 5A and B). Consistent with the previous findings (65, 66), association of Mec1 and Ddc1 with DSBs was partially defective in *rfa1-t11* single mutants. As expected, Mec1 association was further decreased and undetectable in *rfa1-t11 xrs2*Δ double mutants (Fig. 5A). However, introduction of *xrs2*Δ mutation did not affect Ddc1 association with DSBs in *rfa1-t11* mutants (Fig. 5B).

We also monitored the DNA degradation rate at DSB ends in *rfa1-t11 xrs2*Δ mutant cells (Fig. 5C). Cells carrying the GAL-HO plasmid were grown as above to induce *HO* expression. After *HO* expression, cells were collected at various times to prepare genomic DNA. Purified DNA was subjected to blot hybridization analysis. The *rfa1-t11* mutation alone did not affect the rate of 5′ to 3′ degradation of the DNA ends, but introduction of the *rfa1-t11* mutation reduced the degradation rate in *xrs2*Δ mutants. No defect in the 3′ to 5′ degradation was found in *rfa1-t11* single or *rfa1-t11 xrs2*Δ double mutants. These results are consistent with the model in which the generation of long ssDNA tracts promotes Mec1 association with DSBs but not Ddc1 association.

Effect of *xrs2*Δ and *mre11*Δ mutations on cellular responses to UV irradiation. Exposure of cells to UV light results in checkpoint activation, and this UV-induced checkpoint activation depends on Mec1 functions. We thus investigated the effect of *xrs2*Δ and *exo1*Δ mutations on cellular responses to UV irradiation. We first examined the effect of *xrs2*Δ and *exo1*Δ mutations on viability loss after UV irradiation (Fig. 6A). Whereas *xrs2*Δ single mutants were sensitive to UV light, *exo1*Δ single mutants were as resistant as wild-type cells. However, the introduction of *exo1*Δ mutation increased UV sensitivity of *xrs2*Δ mutants. We next monitored UV-induced Rad53 phosphorylation in *xrs2*Δ and *exo1*Δ mutants (Fig. 6B). Cells expressing Rad53-HA were arrested with nocodazole at G_2/M. After arrest, cells were irradiated with UV light and subjected to immunoblotting analysis. Rad53 was phosphorylated in *xrs2*Δ and *exo1*Δ single mutants within 30 min after irradiation, as found in wild-type cells. However, phosphorylation was decreased in *xrs2*Δ *exo1*Δ double mutants: no phosphorylation was observed 30 min after irradiation, although some phosphorylation was detected at later time points. We also monitored Chk1 phosphorylation after UV irradiation (Fig. 6C). Whereas *xrs2*Δ *exo1*Δ double mutation decreased UV-induced phosphorylation, no apparent phosphorylation defect was observed in either of the single mutants. We then examined the G_2/M-phase cell-cycle arrest in *xrs2*Δ and *exo1*Δ mutants after UV irradiation (Fig. 6D). After UV irradiation, both *xrs2*Δ and *exo1*Δ mutants delayed mitotic progression as efficiently as wild-type cells. In contrast, *xrs2*Δ *exo1*Δ double mutants underwent mitosis faster than wild-type cells. To address the effect on activation of the G_1-phase checkpoint pathway, we monitored Rad53 phosphorylation after UV irradiation in G_1-arrested cells (Fig. 6E). Again, Rad53 phosphorylation was significantly decreased in *xrs2*Δ *exo1*Δ double mutants after UV irradiation, whereas no phosphorylation defect was associated with *xrs2*Δ or *exo1*Δ single mutants. Cells containing *mec1* mutations failed to delay mitotic progression and became defective in Rad53 phosphorylation after exposure to UV light, whereas *tel1*Δ mutants did not (50, 58, 59). Thus, the Mre11 complex and Exo1 are functionally overlapped with Mec1 in UV-induced checkpoint responses.

Effect of *xrs2*Δ and *exo1*Δ mutations on checkpoint responses to DNA replication block. Mec1 controls checkpoint responses to DNA replication block as well (11). We therefore addressed whether the Mre11 complex and Exo1 control the replication checkpoint pathway. We first examined HU-induced Rad53 phosphorylation in *xrs2*Δ and *exo1*Δ mutants (Fig. 7A). Cells expressing Rad53-HA were synchronized with α-factor at G_1 and released into medium containing HU. As a control, cells were also released into medium lacking HU. After release, cells were collected at various time points and subjected to immunoblotting analysis. In wild-type and *exo1*Δ single mutant cells, Rad53 was similarly phosphorylated in the presence of HU, whereas no phosphorylation was detected in the absence of HU. Background phosphorylation was detected in *xrs2*Δ single or *xrs2*Δ *exo1*Δ double mutants after release from G_1 arrest. However, HU treatment increased Rad53 phosphorylation more significantly in *xrs2*Δ single mutants compared with *xrs2*Δ *exo1*Δ double mutants. We next monitored cell-cycle arrest in response to DNA replication block (Fig. 7B). Cells were synchronized with α-factor at G_1 and released into medium containing HU. Cells were collected at various time points, and their nuclear and microtubular structures

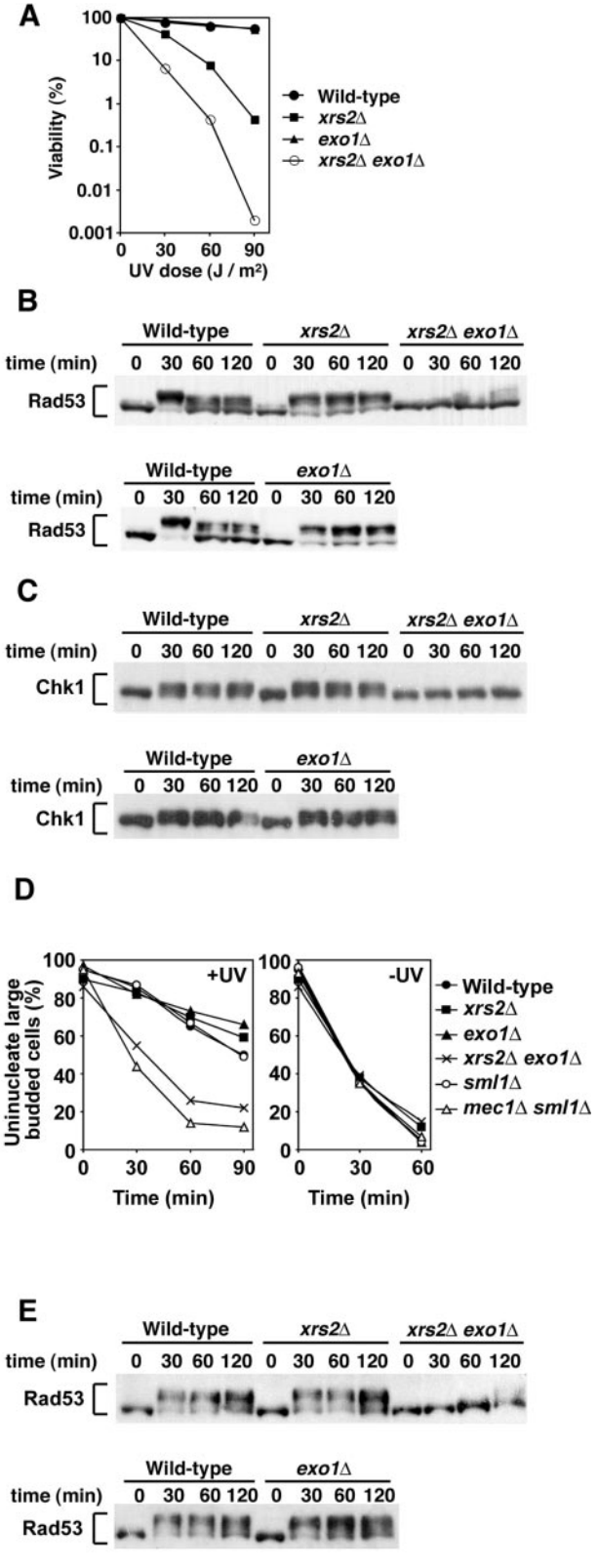

FIG. 6. Redundant role of Xrs2 and Exo1 in cellular responses to UV irradiation. (A) Cell viability after exposure to UV light. Viability was determined after UV irradiation at the indicated dosages. Strains used are the same as in Fig. 2C. (B) Rad53 phosphorylation after UV irradiation at G_2/M. The same cells as in panel A were transformed with YCpT-RAD53-HA. Transformed cells were grown in log phase and treated with nocodazole. After arrest at G_2/M, the culture was irradiated with UV light. Cells were harvested at the indicated times and analyzed as in Fig. 1. (C) Chk1 phosphorylation after UV irradiation at G_2/M. The same cells as in panel A were transformed with YCpT-CHK1-HA and analyzed as in panel B. (D) G_2/M-phase cell cycle progression after exposure to UV light. Cells were grown in YEPD and arrested with nocodazole. After synchronization at G_2/M, cells were irradiated with UV (+UV) or mock-treated (−UV). At the indicated times after release of cultures from nocodazole, the percentage of uninucleate large-budded cells was scored after DAPI staining. Strains used are the same as in Fig. 2D. (E) Rad53 phosphorylation after UV irradiation at G_1. Cells carrying YCpT-RAD53-HA were treated with α-factor. After arrest at G_1, the culture was irradiated with UV light. Cells were harvested at the indicated times and analyzed as in panel B. Strains used are the same as in panel A.

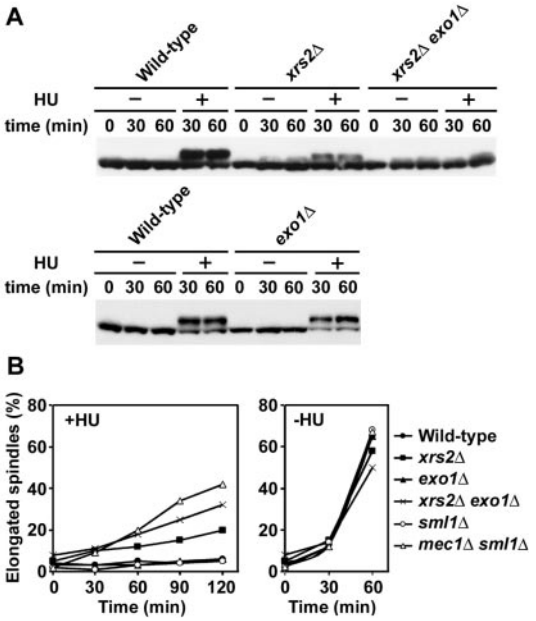

FIG. 7. Effects of *xrs2*Δ and *exo1*Δ mutations on checkpoint responses to DNA replication block. (A) Rad53 phosphorylation after HU treatment. Cells were transformed with YCpT-RAD53-HA. Transformed cells were grown in log phase and treated with α-factor. After arrest at G_1, cells were released into medium with HU (+) or without HU (−). Cells were harvested at the indicated times and analyzed as in Fig. 1. Strains used are the same as in Fig. 2C. (B) Mitotic entry after exposure to HU. Cells were grown in YEPD and arrested with α-factor at G_1. Cells were then released into medium with or without HU. At the indicated times after release, the percentage of cells with elongated spindles was scored after staining with DAPI and antitubulin antibodies. Strains used are the same as in Fig. 2D.

were analyzed by immunofluorescence microscopic analysis. In the presence of HU, most wild-type cells were arrested as large-budded cells with short spindles. Similar efficient arrest was observed in *exo1*Δ single mutants. Although both *xrs2*Δ single and *xrs2*Δ *exo1*Δ double mutants showed defects in blocking mitotic entry after release into HU, *xrs2*Δ *exo1*Δ double mutants were more defective than *xrs2*Δ single mutants. We note that *xrs2*Δ single and *xrs2*Δ *exo1*Δ double mutations partially delayed mitotic entry even in the absence of HU, consistent with the background Rad53 phosphorylation during S-phase progression. These results suggest that the Mre11 com-

plex and Exo1 control activation of the replication checkpoint responses as well.

DISCUSSION

Several studies have established that the Mre11 complex regulates activation of the Tel1 signaling pathway. In this study we demonstrate that the Mre11 complex also controls the Mec1 signaling pathway. The Mre11 complex collaborates with Exo1 in producing long 3′ ssDNA tails at DSB ends and promotes Mec1 association with the DSBs. Activation of the Mec1 signaling pathway requires the functions of the Rad24 and Ddc1 complexes. The Rad24 complex recruits the Ddc1 complex to sites of DNA damage. However, association of Ddc1 with DSBs does not require the generation of long ssDNA tracts. Mec1 is not only required for DSB-induced checkpoint responses but also involved in UV-induced checkpoint responses. Accordingly, the Mre11 complex and Exo1 play an overlapping role in activation in both DSB- and UV-induced checkpoints. The Mre11 complex and Exo1 are also involved in checkpoint responses to stalled DNA replication. Our results suggest that the Mre11 complex and Exo1 collaborate in generating long ssDNA tracts and thereby enable Mec1 to associate with DNA lesions.

Several lines of evidence have indicated that the Mre11 complex controls checkpoint responses after DSB induction (9, 19, 56). Mutations in *MRE11*, *RAD50*, or *XRS2* cause a partial defect in checkpoint responses after γ-irradiation (19). Here we also show that the Mre11 complex contributes in part to checkpoint activation in response to HO-induced DSB or after phleomycin treatment. The Mre11 complex collaborates with Exo1 in DNA damage repair and homologous recombination (34, 54). Interestingly, introduction of *exo1*Δ mutation further impairs the checkpoint responses in *mre11*Δ or *xrs2*Δ mutants, although *exo1*Δ mutation alone does not. Mec1 plays a central role in activation of the checkpoint responses, whereas Tel1 contributes little to the responses (38, 39). Together, these findings indicate that the Mre11 complex and Exo1 control the Mec1 signaling pathway after DSB induction.

DSB ends are primarily degraded by 5′ to 3′ exonuclease activities, and this DSB processing is dependent on the Mre11 complex function (21, 28). We also confirmed overlapping roles of the Mre11 complex and Exo1 in the DNA degradation at DSB ends. Whereas *xrs2*Δ mutation delays the 5′ to 3′ DNA degradation, no apparent degradation delay is associated with *exo1*Δ mutation. However, introduction of the *exo1*Δ mutation enhanced degradation defect in *xrs2*Δ mutants. Little effect on the opposite 3′ to 5′ DNA degradation is observed in these single and double mutants. HO incision occurs similarly in these single and double mutants (54). Thus, the Mre11 complex and Exo1 cooperate in producing long ssDNA tracts at DSB ends. However, other proteins are likely involved in activation of the Mec1 pathway, because some residual 5′ to 3′ degradation is still observed in *xrs2*Δ *exo1*Δ double mutants (34, 54). To understand the link of the Mre11 complex and Exo1 to the Mec1 signaling pathway, we examined Mec1 association with DSBs in the *xrs2*Δ and *exo1*Δ mutants. Mec1 association with DSBs was partially decreased in *xrs2*Δ single mutants compared with wild-type cells, and was undetectable in *xrs2*Δ *exo1*Δ double mutants. Together, these results suggest that the Mre11 complex and Exo1 collaborate in generation of long ssDNA tails at DSB ends, thereby leading to activation of the Mec1 signaling pathway.

DSBs result from breakage of the sugar-phosphate backbone after genotoxic stress. In addition, various adductive DNA products are generated in cells that suffer the effects of genotoxic agents. UV radiation produces two major classes of DNA lesions, the cyclobutane pyrimidine dimers and 6-4 photoproducts (14). The bulky adducts on these photolesions distort the DNA helix and become substrates for nucleotide excision repair (NER) (10). NER is a multistep process that involves bipartite damage recognition, oligonucleotide excision, and gap-filling DNA synthesis (10). Removal of damaged nucleotides, followed by two DNA incisions, leaves single-stranded regions consisting of approximately 24 to 32 nucleotides (10). This ssDNA region might be involved in activation of the Mec1 signaling pathway. Although NER represents a major repair system for UV-induced photoproducts, the NER-independent mechanism contributes to repair of UV-induced lesions as well. Indeed, the Mre11 complex and Exo1 are required for UV-induced damage repair (38, 44). If the ssDNA region could not be filled immediately, endonucleases might cleave the ssDNA region, giving rise to a DSB. This DSB generation might require functions of the Mre11 complex, because Mre11 proteins possess ssDNA endonuclease activities in vitro. In any cases, once generated, DSBs would be processed by the Mre11 complex and Exo1, generating long ssDNA tracts which efficiently recruit Mec1. Alternatively, NER-independent mechanisms might convert UV-induced lesions into DSBs. If the above model were the case, NER dysfunction could also cause a checkpoint defect after UV irradiation, but would not eliminate the checkpoint response. *RAD14* in budding yeast is implicated in the NER pathway (10). Consistently, *rad14*Δ mutations confer a defect in Rad53 phosphorylation immediately after UV irradiation (15), but its phosphorylation becomes detectable at a later time point (62).

DNA replication block after HU treatment activates checkpoint responses in a Mec1-dependent manner. Accordingly, the Mre11 complex and Exo1 are both required for phosphorylation of Rad53 after HU treatment. These results imply that the stalled replication forks are converted to lesions containing DSBs, where the Mre11 complex and Exo1 contribute to generation of long ssDNA tracts. Even in the absence of HU, *xrs2*Δ and *xrs2*Δ *exo1*Δ mutants exhibited a background Rad53 phosphorylation in S phase. In contrast, no apparent background phosphorylation was detected at G_1 or G_2/M phase (for example, see Fig. 2). Thus, the S-phase progression by itself produces DNA lesions in *xrs2*Δ single and *xrs2*Δ *exo1*Δ double mutants. It is possible that DSBs that arise during normal DNA replication are not repaired in *xrs2*Δ mutants (7). The accumulating DSB lesions might be degraded into ssDNAs by nucleases other than the Mre11 complex and Exo1, thereby activating the Mec1 signaling pathway even in the absence of HU.

Activation of the Mec1 signaling pathway also requires functions of Rad24, Ddc1, Mec3, and Rad17. Rad24 (related to human Rad17) forms an RFC-related complex with small subunits of RFC, whereas Ddc1, Mec3, and Rad17 (Rad9, Hus1, and Rad1 in humans) display sequence relatedness to PCNA and form a heterotrimer complex. As RFC loads PCNA on a primer-template junction, the Rad24 (human Rad17) complex loads the Ddc1 (human Rad9) complex on DNA in vitro (3, 12,

31, 66). Consistently, Rad24 recruits the Ddc1 complex to sites of DNA damage in vivo (25, 32). Association of the Ddc1 complex with DNA lesions also requires the function of the ssDNA-binding protein RPA. In fact, Ddc1 association with DSBs is decreased in cells carrying *rfa1-t11*, a mutation in *RFA1* encoding the large subunit of RPA (66). Although the *rfa1-t11* mutation alone does not affect DNA degradation rate at DSBs, introduction of the *rfa1-t11* mutation further delayed ssDNA accumulation in *xrs2*Δ mutants. However, Ddc1 association with DSB in *rfa1-t11 xrs2*Δ double mutants was similar to that in *rfa1-t11* single mutants. Ddc1 association with DSBs does not require generation of long ssDNA tracts; Ddc1 accumulates at DSBs in *xrs2*Δ *exo1*Δ mutants as efficiently as in wild-type cells. RPA thus contributes to aspects other than stabilization of long ssDNA tracts to localize the Ddc1 complex to DNA lesions. More defective DNA degradation was observed in *rfa1-t11 xrs2*Δ double mutants, suggesting that RPA could control the recruitment of nucleases other than the Mre11 complex. The RPA requirement was also examined in vitro using the yeast Ddc1 or human Rad9 complex, but its requirement might depend on the DNA substrate structures (3, 12, 31, 66). Circular DNA substrates with small gaps or nicks can serve as good loading templates for the yeast and human complexes in the absence of RPA (3, 31), whereas circular substrates with extended ssDNA regions require RPA for loading (66). When a linear DNA substrate is used, RPA appears to stimulate loading of the complex on the DNA and inhibit its sliding off from the substrate (12). Thus, RPA plays an important role in loading the Ddc1 complex and its homologs on the DNA substrate, but its biochemical role has not been precisely determined.

Mec1 is involved not only in DNA damage checkpoint but also telomere maintenance (45). Telomeres are shortened in *tel1*Δ mutants compared with wild-type cells (18). Although *mec1*Δ mutation by itself does not affect the telomere length (18), introduction of *mec1*Δ mutation can shorten telomeres in *tel1*Δ mutants (5). The Mre11 complex controls not only the Tel1 pathway (38, 56) but also part of the Mec1 pathway in response to DNA damage. However, the Mre11 complex and Tel1 control the same pathway in maintenance of telomere length (46). Exo1 is required for checkpoint response in *mre11*Δ mutants but dispensable for telomere maintenance in *mre11*Δ mutants (27, 34). One explanation could be that although the Mre11 complex is essential for telomere maintenance, the nuclease activity is not required for the maintenance. There is no good correlation between the length of telomere and ability to process DSB ends among *mre11* mutants (27, 33). Alternatively, proteins other than the Mre11 complex and Exo1 might play a more important role in generation of ssDNA tracts at telomere ends. Although Mec1 is recruited to telomere ends (51), it is not clear whether its localization requires the function of the Mre11 complex or Exo1.

In summary, we provide evidence indicating that the Mre11 complex and Exo1 collaborate in generating long ssDNA tract at sites of DNA damage and promoting Mec1 association with the DNA damage sites. Previous studies have demonstrated that the Mre11 complex is essential for activation of the Tel1 signaling pathway. The Mre11 complex thus governs two separate Mec1 and Tel1 signaling pathways in budding yeast. In mammals, it has been well demonstrated that the Mre11 complex and ATM act in the same DNA damage checkpoint pathway. Recently, however, there is accumulating evidence supporting the theory that the Mre11 complex may control the ATR pathway during DSB metabolism (4). Similar to the Mre11 complex, Exo1 is highly conserved from yeast to humans. It is possible that the Mre11 complex and Exo1 control activation of the ATR signaling pathway through a similar mechanism.

ACKNOWLEDGMENTS

We thank T. Wakayama for plasmid and strain construction and R. Kolodner, H. Ogawa, T. Ogawa, H. Tsubouchi, and K. Umezu for materials. We also thank C. Newlon and her lab members for helpful discussion.

This work was partially supported by the Foundation of UMDNJ.

REFERENCES

1. **Abraham, R. T.** 2001. Cell cycle checkpoint signaling through the ATM and ATR kinases. Genes Dev. **15:**2177–2196.
2. **Bakkenist, C. J., and M. B. Kastan.** 2003. DNA damage activates ATM through intermolecular autophosphorylation and dimer dissociation. Nature **421:**499–506.
3. **Bermudez, V. P., L. A. Lindsey-Boltz, A. J. Cesare, Y. Maniwa, J. D. Griffith, J. Hurwitz, and A. Sancar.** 2003. Loading of the human 9–1–1 checkpoint complex onto DNA by the checkpoint clamp loader hRad17-replication factor C complex in vitro. Proc. Natl. Acad. Sci. USA **100:**1633–1638.
4. **Carson, C. T., R. A. Schwartz, T. H. Stracker, C. E. Lilley, D. V. Lee, and M. D. Weitzman.** 2003. The Mre11 complex is required for ATM activation and the G_2/M checkpoint. EMBO J. **22:**6610–6620.
5. **Chan, S. W., J. Chang, J. Prescott, and E. H. Blackburn.** 2001. Altering telomere structure allows telomerase to act in yeast lacking ATM kinases. Curr. Biol. **11:**1240–1250.
6. **Cortez, D., S. Guntuku, J. Qin, and S. J. Elledge.** 2001. ATR and ATRIP: partners in checkpoint signaling. Science **294:**1713–1716.
7. **Costanzo, V., K. Robertson, M. Bibikova, E. Kim, D. Grieco, M. Gottesman, D. Carroll, and J. Gautier.** 2001. Mre11 protein complex prevents double-strand break accumulation during chromosomal DNA replication. Mol. Cell **8:**137–147.
8. **D'Amours, D., and S. P. Jackson.** 2002. The Mre11 complex: at the crossroads of dna repair and checkpoint signalling. Nat. Rev. Mol. Cell Biol. **3:**317–327.
9. **D'Amours, D., and S. P. Jackson.** 2001. The yeast Xrs2 complex functions in S phase checkpoint regulation. Genes Dev. **15:**2238–2249.
10. **de-Laat, W. L., N. G. Jaspers, and J. H. Hoeijmakers.** 1999. Molecular mechanism of nucleotide excision repair. Genes Dev. **13:**768–785.
11. **Elledge, S. J.** 1996. Cell cycle checkpoints: preventing an identity crisis. Science **274:**1664–1672.
12. **Ellison, V., and B. Stillman.** 2003. Biochemical characterization of DNA damage checkpoint complexes: clamp loader and clamp complexes with specificity for 5′ recessed DNA. PLoS Biol. **1:**E33.
13. **Fiorentini, P., K. N. Huang, D. X. Tishkoff, R. D. Kolodner, and L. S. Symington.** 1997. Exonuclease I of *Saccharomyces cerevisiae* functions in mitotic recombination in vivo and in vitro. Mol. Cell. Biol. **17:**2764–2773.
14. **Friedberg, E. C., G. C. Walker, and W. Siede.** 1995. DNA repair and mutagenesis. ASM Press, Washington, D.C.
15. **Giannattasio, M., F. Lazzaro, M. P. Longhese, P. Plevani, and M. Muzi-Falconi.** 2004. Physical and functional interactions between nucleotide excision repair and DNA damage checkpoint. EMBO J. **23:**429–438.
16. **Gietz, R. D., and A. Sugino.** 1988. New yeast-*Escherichia coli* shuttle vectors constructed with in vitro mutagenized yeast genes lacking six-base pair restriction sites. Gene **74:**527–534.
17. **Green, C. M., H. Erdjument-Bromage, P. Tempst, and N. F. Lowndes.** 2000. A novel Rad24 checkpoint protein complex closely related to replication factor C. Curr. Biol. **10:**39–42.
18. **Greenwell, P. W., S. L. Kronmal, S. E. Porter, J. Gassenhuber, B. Obermaier, and T. D. Petes.** 1995. *TEL1*, a gene involved in controlling telomere length in *S. cerevisiae*, is homologous to the human ataxia telangiectasia gene. Cell **82:**823–829.
19. **Grenon, M., C. Gilbert, and N. F. Lowndes.** 2001. Checkpoint activation in response to double-strand breaks requires the Mre11/Rad50/Xrs2 complex. Nat. Cell Biol. **3:**844–847.
20. **Haber, J. E.** 1998. The many interfaces of Mre11. Cell **95:**583–586.
21. **Ivanov, E. L., N. Sugawara, C. I. White, F. Fabre, and J. E. Haber.** 1994. Mutations in *XRS2* and *RAD50* delay but do not prevent mating-type switching in *Saccharomyces cerevisiae*. Mol. Cell. Biol. **14:**3414–3425.
22. **Kastan, M. B., and D. S. Lim.** 2000. The many substrates and functions of ATM. Nat. Rev. Mol. Cell Biol. **1:**179–186.
23. **Katou, Y., Y. Kanoh, M. Bando, H. Noguchi, H. Tanaka, T. Ashikari, K.**

Sugimoto, and K. Shirahige. 2003. S-phase checkpoint proteins Tof1 and Mrc1 form a stable replication-pausing complex. Nature **424:**1073–1083.
24. **Kitagawa, R., C. J. Bakkenist, P. J. McKinnon, and M. B. Kastan.** 2004. Phosphorylation of SMC1 is a critical downstream event in the ATM-NBS1-BRCA1 pathway. Genes Dev. **18:**1423–1438.
25. **Kondo, T., T. Wakayama, T. Naiki, K. Matsumoto, and K. Sugimoto.** 2001. Recruitment of Mec1 and Ddc1 checkpoint proteins to double-strand breaks through distinct mechanisms. Science **5543:**867–870.
26. **Lee, J. H., and T. T. Paull.** 2004. Direct activation of the ATM protein kinase by the Mre11/Rad50/Nbs1 complex. Science **304:**93–96.
27. **Lee, S. E., D. A. Bressan, J. H. Petrini, and J. E. Haber.** 2002. Complementation between N-terminal *Saccharomyces cerevisiae mre11* alleles in DNA repair and telomere length maintenance. DNA Repair (Amsterdam) **1:**27–40.
28. **Lee, S. E., J. K. Moore, A. Holmes, K. Umezu, R. D. Kolodner, and J. E. Haber.** 1998. *Saccharomyces* Ku70, Mre11/Rad50 and RPA proteins regulate adaptation to G_2/M arrest after DNA damage. Cell **94:**399–409.
29. **Longhese, M. P., M. Foiani, M. Muzi-Falconi, G. Lucchini, and P. Plevani.** 1998. DNA damage checkpoint in budding yeast. EMBO J. **17:**5525–5528.
30. **Lucca, C., F. Vanoli, C. Cotta-Ramusino, A. Pellicioli, G. Liberi, J. Haber, and M. Foiani.** 2004. Checkpoint-mediated control of replisome-fork association and signalling in response to replication pausing. Oncogene **23:**1206–1213.
31. **Majka, J., and P. M. Burgers.** 2003. Yeast Rad17/Mec3/Ddc1: a sliding clamp for the DNA damage checkpoint. Proc. Natl. Acad. Sci. USA **100:**2249–2254.
32. **Melo, J. A., J. Cohen, and D. P. Toczyski.** 2001. Two checkpoint complexes are independently recruited to sites of DNA damage in vivo. Genes Dev. **21:**2809–2821.
33. **Moreau, S., J. R. Ferguson, and L. S. Symington.** 1999. The nuclease activity of Mre11 is required for meiosis but not for mating type switching, end joining, or telomere maintenance. Mol. Cell. Biol. **19:**556–566.
34. **Moreau, S., E. A. Morgan, and L. S. Symington.** 2001. Overlapping functions of the Saccharomyces cerevisiae Mre11, Exo1 and Rad27 nucleases in DNA metabolism. Genetics **159:**1423–1433.
35. **Morrow, D. M., D. A. Tagle, Y. Shiloh, F. S. Collins, and P. Hieter.** 1995. TEL1, an S. cerevisiae homolog of the human gene mutated in ataxia telangiectasia, is functionally related to the yeast checkpoint gene, MEC1. Cell **82:**831–840.
36. **Naiki, T., T. Shimomura, T. Kondo, K. Matsumoto, and K. Sugimoto.** 2000. Rfc5, in cooperation with Rad24, controls DNA damage checkpoints throughout the cell cycle in *Saccharomyces cerevisiae*. Mol. Cell. Biol. **20:**5888–5896.
37. **Naiki, T., T. Wakayama, D. Nakada, K. Matsumoto, and K. Sugimoto.** 2004. Association of Rad9 with double-strand breaks through a Mec1-dependent mechanism. Mol. Cell. Biol. **24:**3277–3285.
38. **Nakada, D., K. Matsumoto, and K. Sugimoto.** 2003. ATM-related Tel1 associates with double-strand breaks through an Xrs2-dependent mechanism. Genes Dev. **17:**1957–1962.
39. **Nakada, D., T. Shimomura, K. Matsumoto, and K. Sugimoto.** 2003. The ATM-related Tel1 protein of *Saccharomyces cerevisiae* controls a checkpoint response following phleomycin treatment. Nucleic Acids Res. **31:**1715–1724.
40. **Osborn, A. J., and S. J. Elledge.** 2003. Mrc1 is a replication fork component whose phosphorylation in response to DNA replication stress activates Rad53. Genes Dev. **17:**1755–1767.
41. **Paciotti, V., M. Clerici, G. Lucchini, and M. P. Longhese.** 2000. The checkpoint protein Ddc2, functionally related to *S. pombe* Rad26, interacts with Mec1 and is regulated by Mec1-dependent phosphorylation in budding yeast. Genes Dev. **14:**2046–2059.
42. **Pellicioli, A., S. E. Lee, C. Lucca, M. Foiani, and J. E. Haber.** 2001. Regulation of Saccharomyces Rad53 checkpoint kinase during adaptation from DNA damage-induced G_2/M arrest. Mol. Cell **7:**293–300.
43. **Petrini, J. H.** 2000. The Mre11 complex and ATM: collaborating to navigate S phase. Curr. Opin. Cell Biol. **12:**293–296.
44. **Qiu, J., M. X. Guan, A. M. Bailis, and B. Shen.** 1998. *Saccharomyces cerevisiae* exonuclease-1 plays a role in UV resistance that is distinct from nucleotide excision repair. Nucleic Acids Res. **26:**3077–3783.
45. **Ritchie, K. B., J. C. Mollory, and T. D. Petes.** 1999. Interactions of *TLC1* (which encodes the RNA subunit of telomerase), *TEL1*, and *MEC1* in regulating telomere length in the yeast *Saccharomyces cerevisiae*. Mol. Cell. Biol. **19:**6065–6075.
46. **Ritchie, K. B., and T. D. Petes.** 2000. The Mre11p/Rad50p/Xrs2p complex and the Tel1p function in a single pathway for telomere maintenance in yeast. Genetics **155:**475–479.
47. **Rouse, J., and S. P. Jackson.** 2000. *LCD1*: an essential gene involved in checkpoint control and regulation of the *MEC1* signalling pathway in *Saccharomyces cerevisiae*. EMBO J. **19:**5793–5800.
48. **Rouse, J., and S. P. Jackson.** 2002. Lcd1p recruits Mec1p to DNA lesions in vitro and in vivo. Mol. Cell **9:**857–869.
49. **Sanchez, Y., J. Bachant, H. Wang, F. Hu, D. Liu, M. Tetzlaff, and S. J. Elledge.** 1999. Control of the DNA damage checkpoint by chk1 and rad53 protein kinases through distinct mechanisms. Science **286:**1166–1171.
50. **Sanchez, Y., B. A. Desany, W. J. Jones, Q. Liu, B. Wang, and S. J. Elledge.** 1996. Regulation of *RAD53* by the *ATM*-like kinase *MEC1* and *TEL1* in yeast cell cycle checkpoint pathways. Science **271:**357–360.
51. **Takata, H., Y. Kanoh, N. Gunge, K. Shirahige, and A. Matsuura.** 2004. Reciprocal association of the budding yeast ATM-related proteins Tel1 and Mec1 with telomeres in vivo. Mol. Cell **14:**515–522.
52. **Tishkoff, D. X., N. S. Amin, C. S. Viars, K. C. Arden, and R. D. Kolodner.** 1998. Identification of a human gene encoding a homologue of Saccharomyces cerevisiae EXO1, an exonuclease. Cancer Res. **58:**5027–5031.
53. **Toczyski, D. P., D. J. Galgoczy, and L. H. Hartwell.** 1997. *CDC5* and CKII control adaptation to the yeast DNA damage checkpoint. Cell **90:**1097–1106.
54. **Tsubouchi, H., and H. Ogawa.** 2000. Exo1 roles for repair of DNA double-strand breaks and meiotic crossing over in *Saccharomyces cerevisiae*. Mol. Biol. Cell **11:**2221–2233.
55. **Umezu, K., N. Sugawara, C. Chen, J. E. Haber, and R. D. Kolodner.** 1998. Genetic analysis of yeast RPA1 reveals its multiple functions in DNA metabolism. Genetics **148:**989–1005.
56. **Usui, T., H. Ogawa, and J. H. Petrini.** 2001. A DNA damage response pathway controlled by Tel1 and the Mre11 complex. Mol. Cell **7:**1255–1266.
57. **Uziel, T., Y. Lerenthal, L. Moyal, Y. Andegeko, L. Mittelman, and Y. Shiloh.** 2003. Requirement of the MRN complex for ATM activation by DNA damage. EMBO J. **22:**5612–5621.
58. **Vialard, J. E., C. S. Gilbert, C. M. Green, and N. F. Lowndes.** 1998. The budding yeast Rad9 checkpoint protein is subjected to Mec1/Tel1-dependent hyperphosphorylation and interacts with Rad53 after DNA damage. EMBO J. **17:**5679–5688.
59. **Wakayama, T., T. Kondo, S. Ando, K. Matsumoto, and K. Sugimoto.** 2001. Pie1, a protein interacting with Mec1, controls cell growth and checkpoint responses in *Saccharomyces cerevisiae*. Mol. Cell. Biol. **21:**755–764.
60. **White, C. I., and J. E. Haber.** 1990. Intermediates of recombination during mating type switching in *Saccharomyces cerevisiae*. EMBO J. **9:**663–673.
61. **Wold, M. S.** 1997. Replication protein A: a heterotrimeric, single-stranded DNA-binding protein required for eukaryotic DNA metabolism. Annu. Rev. Biochem. **66:**61–92.
62. **Zhang, H., J. Taylor, and W. Siede.** 2003. Checkpoint arrest signaling in response to UV damage is independent of nucleotide excision repair in *Saccharomyces cerevisiae*. J. Biol. Chem. **278:**9382–9387.
63. **Zhao, X., E. G. D. Muller, and R. Rothstein.** 1998. A suppressor of two essential checkpoint genes identifies a novel protein that negatively affects dNTP pool. Mol. Cell **2:**329–340.
64. **Zhou, B.-B. S., and S. J. Elledge.** 2000. The DNA damage response: putting checkpoints in perspective. Nature **408:**433–439.
65. **Zou, L., and S. J. Elledge.** 2003. Sensing DNA damage through ATRIP recognition of RPA-ssDNA complexes. Science **300:**1542–1548.
66. **Zou, L., D. Liu, and S. J. Elledge.** 2003. Replication protein A-mediated recruitment and activation of Rad17 complexes. Proc. Natl. Acad. Sci. USA **100:**13827–13832.